

Published in final edited form as:

Biochem Biophys Res Commun. 2009 May 29; 383(2): 198–202. doi:10.1016/j.bbrc.2009.03.151.

Cd²⁺, Mn²⁺, Ni²⁺ and Se²⁺ toxicity to *Saccharomyces cerevisiae* lacking YPK9p the orthologue of human ATP13A2

Karyn Schmidt¹, Devin M Wolfe¹, Barbara Stiller^{4,5}, and David A Pearce^{1,2,3,*}

¹Center for Neural Development and Disease, University of Rochester School of Medicine and Dentistry, Rochester, New York 14642

²Aab Institute of Biomedical Sciences, Department of Biochemistry and Biophysics, University of Rochester School of Medicine and Dentistry, Rochester, New York 14642

³Department of Neurology, University of Rochester School of Medicine and Dentistry, Rochester, New York 14642

⁴Institute of Human Genetics, University of Cologne, Cologne, Germany

⁵Institute for Genetics, University of Cologne, Cologne, Germany

Abstract

The *Saccharomyces cerevisiae* gene *YPK9* encodes a putative integral membrane protein which is 58% similar and 38% identical in amino acid sequence to the human lysosomal P_{5B} ATPase ATP13A2. Mutations in *ATP13A2* have been found in patients with Kufor-Rakeb syndrome, a form of juvenile Parkinsonism. We report that Ypk9p localizes to the yeast vacuole and that deletion of *YPK9* confers sensitivity for growth for cadmium, manganese, nickel or selenium. These results suggest that Ypk9p may play a role in sequestration of divalent heavy metal ions. Further studies on the function of Ypk9p/ATP13A2 may help to define the molecular basis of Kufor-Rakeb syndrome and provide a potential link to environmental factors such as heavy metals contributing to some forms of Parkinsonism.

Introduction

Kufor Rakeb syndrome (KRS) is a rare form of juvenile Parkinsonism that follows autosomal recessive inheritance, first described in 1994 by Al-Din *et al.* Manifesting between seven and 24 years of age, these patients present with juvenile-onset parkinsonian symptoms attributed to pallido-pyramidal syndrome (PPS), including bradykinesia, paraparesis, stooped posture and hyperreflexia (Davison, 1954; Jankovic, 1989; Nisipeanu, *et al.*, 1994). Kufor Rakeb patients also have distinct symptoms including widespread neurodegeneration resulting in dementia and upgaze paresis, yet lack the intention tremor typical to parkinsonism disorders (al-Din, *et al.*, 1994; Davison, 1954; Hunt, 1917; Nisipeanu, *et al.*, 1994; Williams, *et al.*, 2005). The causative gene associated with KRS is *ATP13A2*. *ATP13A2* encodes an 1180 amino acid P-type ATPase, specifically of the P₅ subfamily, that localizes to the lysosome (Axelsen and Palmgren, 1998; Kuhlbrandt, 2004;

© 2009 Elsevier Inc. All rights reserved.

*Corresponding author: David A. Pearce, PhD, 601 Elmwood Ave, Box 645, Rochester, NY 14620, Phone: 585 273-1509, Fax: 585 276-1972, David_Pearce@urmc.rochester.edu.

Publisher's Disclaimer: This is a PDF file of an unedited manuscript that has been accepted for publication. As a service to our customers we are providing this early version of the manuscript. The manuscript will undergo copyediting, typesetting, and review of the resulting proof before it is published in its final citable form. Please note that during the production process errors may be discovered which could affect the content, and all legal disclaimers that apply to the journal pertain.

Ramirez, et al., 2006). There are several mutations identified with various forms of KRS (Di Fonzo, et al., 2007; Lin, et al., 2008; Ramirez, et al., 2006).

Ypk9p (*YOR291w*) is the *Saccharomyces cerevisiae* homologue to human *ATP13A2* based on amino acid sequence alignment. Ypk9p is a 1472 amino acid P₅ ATPase and has 58% similarity and 38% identity to *ATP13A2*. Recently, Ypk9p was shown to suppress α -synuclein and manganese toxicity in yeast, revealing a connection between the yeast gene and PD genetic and environmental risk factors (Gitler, et al., 2009). We demonstrate that deletion of *YPK9*, *ypk9-Δ*, results in sensitivity to cadmium, manganese, nickel and selenium. Further studies of the yeast protein may help to elucidate the function of *ATP13A2* and uncover underlying defects of Kufor Rakeb syndrome.

Materials and Methods

Strains and plasmid construction

The parental (*MATahis3Δ1 leu2Δ0 lys2Δ0 ura3Δ0*) and single deletion strains used in this study were purchased from Open BioSystems. *YPK9-GST* in pEGH was purchased from Open Biosystems and transformed into *ypk9-Δ* using standard lithium acetate transformation protocol (Ito, et al., 1983; Schiestl and Gietz, 1989). *ATP13A2* was amplified from human cDNA and subcloned into pcDNA3.1 (Invitrogen) and ligated into pYeura3 (Clontech) and transformed into *YPK9⁺* and *ypk9-Δ* strains. *YPK9-GFP* was purchased from Invitrogen (Huh, et al., 2003).

Media and growth conditions

Rich media (YPD) contained 1% yeast extract, 2% peptone and 2% dextrose. Synthetic complete (SC) media contains 6.7 mg/ml yeast nitrogen base without amino acids, 5 mg/ml ammonium sulfate, 2% dextrose and all essential amino acids. Strains transformed with plasmids were selected and maintained on synthetic complete media lacking uracil (SC-ura). Galactose inducible plasmids were induced in SC-ura media containing 2% galactose and 0.1% raffinose in place of dextrose. Filter sterilized metal solutions were added to the appropriate concentration to either YPD or SC media after autoclaving.

Serial Dilutions

Strains were grown overnight in SC-ura media, harvested and washed twice in sterile water, re-inoculated and induced in 2% galactose media. Uninduced control strains were grown overnight in either YPD or SC-ura media. Strains were then harvested, washed twice, and resuspended at 3×10^8 cells/ml. Strains were serially diluted 10-fold. Cells were transferred to media with a 36-pin replicator, and plates were incubated at 30°C or 37°C for 3-5 days.

Colocalization of YPK9 with FM4-64

YPK9 tagged with green fluorescent protein (Invitrogen) was grown to log-phase in YPD, harvested, washed twice in 1 ml SC media, and resuspended in 100μl of SC media. FM4-64 staining was performed as previously described by Vida and Emr (Vida and Emr, 1995). Photomicrographs were obtained using an Axioplan2 Epifluorescent microscope. Cells were visualized under the 100× objective using an Epifluorescent microscope (Olympus BX61, Melville, NY), a CoolSNAP HQ CCD camera (Photometrics, Tucson, AR), and IPLab 4.0 acquisition software (BD Bioscience, Rockville, MD). Post imaging processing was performed using Autoquant X2 (Media Cybernetics). Image deconvolution was performed using the Autodeblur software package (Media Cybernetics, Bethesda, MD) and overlays of fluorescent images were performed using ImageJ software (NIH).

Results

Identification of YPK9

YOR291w is the yeast homolog to human *ATP13A2* (58% similarity and 38% identity). *ATP13A2* and Ypk9p both contain a PPALP sequence at the proposed ion binding site, classifying them as P₅ ATPases of the P_{5B} subfamily (Moller, et al., 2008). Spf1p, the other yeast P-type ATPase, is classified as a P_{5A} ATPase and is presumed to have different ion specificities from Ypk9p based on the presence of 2 negative charges in place of the hydrophobic residue in P_{5B} ATPases (Moller, et al., 2008). There appears to be some functional overlap between the two yeast P-type ATPases, however, as overexpression of YPK9 is able to rescue the a-syn toxicity seen in *spf1-Δ* (Gitler, et al., 2009).

Cadmium, manganese, nickel, and selenium are toxic to *ypk9-Δ* cells

P-type ATPases hydrolyze ATP to maintain an ion gradient across a membrane. We therefore compared growth for serial dilutions of *YPK9*⁺ and *ypk9-Δ* cells on media containing various dibasic metals. Sublethal metal concentrations were used or modified from a previous study (Table 1) (Pearce and Sherman, 1999). All strains were plated on unsupplemented YPD to determine a standard level of growth (Figure 1). *ypk9-Δ* exhibited growth defects when grown at 30° on YPD containing 8μM cadmium, 3mM manganese, 2.5mM nickel or 0.7mM selenium (Figure 1 and 2). Growth defects were also evident on YPD supplemented with these metals at 37° and SC media at both 30° and 37° (data not shown). Plasmid borne expression of *YPK9* complemented these phenotypes (Figure 2). The function of a GFP tagged Ypk9p was also tested. There was a small growth defect of the GFP tagged Ypk9p on all 4 of the metal supplemented media, indicating that the construct is only partially functional (Figure 3). Human *ATP13A2* does not appear to complement the *ypk9-Δ* phenotype (Figure 2).

YPK9p localizes to the vacuole

ATP13A2 localizes to the lysosome. Ypk9p-GFP co-localizes with the steryl dye FM4-64, indicating that Ypk9p is a vacuolar membrane protein, which is analogous to the mammalian lysosomal membrane (Figure 3). This confirms vacuolar localization of Ypk9-GFP (Gitler, et al., 2009).

Histidine metabolism affects toxicity of nickel and selenium in *ypk9-Δ* cells

In yeast the ability to synthesize histidine increases resistance to copper, cobalt and nickel salts (Farcasanu, et al., 2005; Pearce and Sherman, 1999). As our strains are histidine auxotrophs, due to the presence of *his3ΔI*, we tested if complementation with the *HIS3* gene on the centromeric plasmid, pRS313, conferred tolerance to cadmium, manganese, nickel or selenium in *ypk9-Δ*. Toxicity of nickel and selenium in *ypk9-Δ* was partially suppressed by expression of *HIS3* (Figure 4), as well as YPK9 (Figure 2).

Discussion

YPK9 is the yeast homolog of human gene *ATP13A2*, which is mutated in Kufor Rakeb syndrome patients. Our results suggest that Ypk9p could play a role in resistance to cadmium, manganese, nickel and selenium in the vacuole. However, nickel and selenium resistance may be influenced by the status of histidine metabolism. The sensitivity of *ypk9-Δ* to these metals may result from the inability of the cells to sequester the surplus of metals in the vacuole, thereby increasing cytosolic concentrations to toxic levels.

Cadmium and nickel are known cellular toxicants that increase reactive oxygen species (ROS) in cells. Both metals bind to sulfhydryl groups, common in antioxidants and other

enzymes which reduce ROS. The binding of cadmium or nickel results in the inactivation of these enzymes and a consequent increase in ROS (Das, et al., 2008; Ercal, et al., 2001; Jarup, et al., 1998). Cadmium and nickel also inhibit yeast glutathione/reductase, the enzyme responsible for the reduction of oxidized glutathione (GSSH) to reduced glutathione (GSH) (Tandogan and Ulusu, 2007). GSH is the required substrate for glutathione peroxidase, which couples the reduction of H₂O₂ to H₂O with the oxidation of GSH to GSSH. Cadmium and nickel therefore pose a double threat to antioxidant mechanisms in the cell, as they can either directly inhibit critical antioxidants or deplete glutathione levels necessary for the function of these enzymes. Additionally, cadmium has an inhibitory effect on complex III of the mitochondrial electron transport chain (Miccadei and Floridi, 1993; Wang, et al., 2004). Inhibition of this complex specifically stops electron transport to cytochrome C, resulting in the formation of ROS.

Since cadmium and nickel are not essential ions, specific importers for these metals are not reported and they most likely enter cells nonspecifically through other essential metal ion transporters. For example, cadmium has been shown to enter cells through divalent metal transporter (DMT1), iron transporters and zinc transporters, as well as through calcium channels (Bressler, et al., 2004; Dalton, et al., 2005; Gomes, et al., 2002; Leslie, et al., 2006; Perfus-Barbeoch, et al., 2002). The cadmium-transporting P_{1B}-type ATPase in *Saccharomyces cerevisiae*, Pca1p, has been shown to be crucial for cadmium efflux. Interestingly, the gene has been shown to contain a mutation in several common laboratory strains, including the strain used in this study, which renders the protein nonfunctional (Adle and Lee, 2008). If Pca1p works in tandem with Ypk9p, the deletion of *ypk9* from a strain already containing a nonfunctional cadmium efflux transporter would render the cells unable to purge cadmium through either ATPase, resulting in the toxicity we see here.

Selenium binds in the active site of glutathione peroxidase (GPx), the enzyme responsible for the reduction of H₂O₂ to H₂O (Li, et al., 1990; Rotruck, et al., 1973). A positive correlation is seen between GPx activity and selenium uptake, resulting in an increase in resistance to oxidative damage (Aguilar, et al., 1998; Castano, et al., 1993; Huang, et al., 1994; Zafar, et al., 2003). Yeast do not encode a classical GPx; rather they contain 3 phospholipid hydroperoxide glutathione peroxidase-like enzymes, denoted Gpx1, 2 and 3, which are selenium independent. Gpx3p acts as a redox-transducer in the presence of hydroperoxide and signals to transcription factor Yap1p, which can also be activated by cadmium and selenium independently of GPx3 (Azevedo, et al., 2003; Delaunay, et al., 2002). A selenium transporter has not been identified in *S. cerevisiae*; however, selenium accumulates primarily in the vacuole, suggesting the presence of such a pump (Gharieb and Gadd, 1998). It is important to note that the deletion of either *yap1* or *gpx3* results in sensitivity to cadmium and selenium, indicating that both of these play a role in protecting the cell against the toxicity of these metals. This also implies the existence of a functional link between Yap1p, Gpx3, and Ypk9p.

Manganese enters *S. cerevisiae* through the divalent metal ion transporter Smf2p and is required as a cofactor for the mitochondrial superoxide dismutase SOD2, a key protectant against mitochondrial oxidative stress (Ravindranath and Fridovich, 1975; Weisiger and Fridovich, 1973). It has been shown that binding of the metal ion to the enzyme occurs in the mitochondrial, presumably because cytosolic concentrations of manganese are too low to activate Sod2p (Luk, et al., 2005). The low cytosolic concentration indicates that either the majority of the ion accumulates in the mitochondria or else other organelles have sequestered the remaining manganese. The protein Ccc1p may sequester manganese to the golgi (Lapinskas, et al., 1996). Currently there is no identified vacuolar manganese transporter, although sequestration here remains likely.

Oxidative stress has been implicated as a pathogenic pathway in many neurodegenerative diseases, including Parkinsons Disease (PD), via its contribution to programmed cell death through the disruption of protein and mitochondrial function (Andersen, 2004). Moreover, evidence suggests that elevated levels of metal ions could lead to oxidative stress, with cadmium, manganese, and selenium being cited as possible examples (Barnham, et al., 2004; Zecca, et al., 2004).

The sequence similarity between the human ATP13A2 and Ypk9p suggest that the two proteins may be functionally related. Mutations in ATP13A2 result in Kufor-Rakeb syndrome. While the function of ATP13A2 still needs to be determined, it is plausible to suggest that it is a transporter for an unidentified cation. Compromised function of ATP13A2 may disrupt the balance of this essential divalent cation. In addition, competition with this divalent cation from other metal ions may provide additional disease burden. Moreover, normal ATP13A2 activity could be compromised upon exposure to certain metal ions providing a potential link to the environment and PD.

Acknowledgments

This work was supported in part by NIH R01 NS36610 and P30 ES01247.

References

- Adle DJ, Lee J. Expressional control of a cadmium-transporting P1B-type ATPase by a metal sensing degradation signal. *J Biol Chem.* 2008; 283:31460–8. [PubMed: 18753133]
- Aguilar MV, Jimenez-Jimenez FJ, Molina JA, Meseguer I, Mateos-Vega CJ, Gonzalez-Munoz MJ, de Bustos F, Gomez-Escalonilla C, Ort-Pareja M, Zurdo M, Martinez-Para MC. Cerebrospinal fluid selenium and chromium levels in patients with Parkinson's disease. *J Neural Transm.* 1998; 105:1245–51. [PubMed: 9928893]
- al-Din SN, Anderson M, Eeg-Olofsson O, Trontelj JV. Neuro- ophthalmic manifestations of the syndrome of ophthalmoplegia, ataxia and areflexia: a review. *Acta Neurol Scand.* 1994; 89:157–63. [PubMed: 8030396]
- Andersen JK. Oxidative stress in neurodegeneration: cause or consequence? *Nat Med.* 2004; 10 Suppl:S18–25. [PubMed: 15298006]
- Axelsen KB, Palmgren MG. Evolution of substrate specificities in the P-type ATPase superfamily. *J Mol Evol.* 1998; 46:84–101. [PubMed: 9419228]
- Azevedo D, Tacnet F, Delaunay A, Rodrigues-Pousada C, Toledano MB. Two redox centers within Yap1 for H₂O₂ and thiol-reactive chemical signaling. *Free Radic Biol Med.* 2003; 35:889–900. [PubMed: 14556853]
- Barnham KJ, Masters CL, Bush AI. Neurodegenerative diseases and oxidative stress. *Nat Rev Drug Discov.* 2004; 3:205–14. [PubMed: 15031734]
- Bressler JP, Olivi L, Cheong JH, Kim Y, Bannona D. Divalent metal transporter 1 in lead and cadmium transport. *Ann N Y Acad Sci.* 2004; 1012:142–52. [PubMed: 15105261]
- Castano A, Cano J, Machado A. Low selenium diet affects monoamine turnover differentially in substantia nigra and striatum. *J Neurochem.* 1993; 61:1302–7. [PubMed: 8376988]
- Dalton TP, He L, Wang B, Miller ML, Jin L, Stringer KF, Chang X, Baxter CS, Nebert DW. Identification of mouse SLC39A8 as the transporter responsible for cadmium-induced toxicity in the testis. *Proc Natl Acad Sci U S A.* 2005; 102:3401–6. [PubMed: 15722412]
- Das KK, Das SN, Dhundasi SA. Nickel, its adverse health effects & oxidative stress. *Indian J Med Res.* 2008; 128:412–25. [PubMed: 19106437]
- Davison C. Pallido-pyramidal disease. *J Neuropathol Exp Neurol.* 1954; 13:50–9. [PubMed: 13118374]
- Delaunay A, Pflieger D, Barrault MB, Vinh J, Toledano MB. A thiol peroxidase is an H₂O₂ receptor and redox-transducer in gene activation. *Cell.* 2002; 111:471–81. [PubMed: 12437921]

- Di Fonzo A, Chien HF, Socal M, Giraudo S, Tassorelli C, Iliceto G, Fabbrini G, Marconi R, Fincati E, Abbruzzese G, Marini P, Squitieri F, Horstink MW, Montagna P, Libera AD, Stocchi F, Goldwurm S, Ferreira JJ, Meco G, Martignoni E, Lopiano L, Jardim LB, Oostra BA, Barbosa ER, Bonifati V. ATP13A2 missense mutations in juvenileparkinsonism and young onset Parkinson disease. *Neurology*. 2007; 68:1557–62. [PubMed: 17485642]
- Ercal N, Gurer-Orhan H, Aykin-Burns N. Toxic metals and oxidativestress part I: mechanisms involved in metal-induced oxidative damage. *Curr Top Med Chem*. 2001; 1:529–39. [PubMed: 11895129]
- Farcasanu IC, Mizunuma M, Nishiyama F, Miyakawa T. Role of L-histidine in conferring tolerance to Ni²⁺ in *Sacchomyces cerevisiae* cells. *Biosci Biotechnol Biochem*. 2005; 69:2343–8. [PubMed: 16377892]
- Gharieb MM, Gadd GM. Evidence for the involvement of vacuolaractivity in metal(loid) tolerance: vacuolar-lacking and -defective mutants of *Saccharomyces cerevisiae* display higher sensitivity to chromate, tellurite and selenite. *Biometals*. 1998; 11:101–6. [PubMed: 9542063]
- Gitler AD, Chesi A, Geddie ML, Strathearn KE, Hamamichi S, Hill KJ, Caldwell KA, Caldwell GA, Cooper AA, Rochet JC, Lindquist S. alpha-Synuclein is part of a diverse and highly conserved interactionnetwork that includes PARK9 and manganese toxicity. *Nat Genet*. 2009
- Gomes DS, Fragoso LC, Riger CJ, Panek AD, Eleutherio EC. Regulation of cadmium uptake by *Saccharomyces cerevisiae*. *Biochim Biophys Acta*. 2002; 1573:21–5. [PubMed: 12383937]
- Huang K, Lauridsen E, Clausen J. The uptake of Na-selenite in rat brain. Localization of new glutathione peroxidases in the rat brain. *Biol Trace Elem Res*. 1994; 46:91–102. [PubMed: 7534099]
- Huh WK, Falvo JV, Gerke LC, Carroll AS, Howson RW, Weissman JS, O'Shea EK. Global analysis of protein localization in budding yeast. *Nature*. 2003; 425:686–91. [PubMed: 14562095]
- Hunt RH. Correspondence. *Cal State J Med*. 1917; 15:474–5. [PubMed: 18737462]
- Ito H, Fukuda Y, Murata K, Kimura A. Transformation of intact yeastcells treated with alkali cations. *J Bacteriol*. 1983; 153:163–8. [PubMed: 6336730]
- Jankovic J. Parkinsonism-plus syndromes. *Mov Disord*. 1989; 4 Suppl 1:S95–119. [PubMed: 2657411]
- Jarup L, Berglund M, Elinder CG, Nordberg G, Vahter M. Health effects of cadmium exposure--a review of the literature and a risk estimate. *Scand J Work Environ Health*. 1998; 24 Suppl 1:1–51. [PubMed: 9569444]
- Kuhlbrandt W. Biology, structure and mechanism of P-type ATPases. *Nat Rev Mol Cell Biol*. 2004; 5:282–95. [PubMed: 15071553]
- Lapinskas PJ, Lin SJ, Culotta VC. The role of the *Saccharomyces cerevisiae* CCC1 gene in the homeostasis of manganese ions. *Mol Microbiol*. 1996; 21:519–28. [PubMed: 8866476]
- Leslie EM, Liu J, Klaassen CD, Waalkes MP. Acquired cadmiumresistance in metallothionein-I/II(-/-) knockout cells: role of the T-type calciumchannel Ca_v1.3 in cadmium uptake. *Mol Pharmacol*. 2006; 69:629–39. [PubMed: 16282520]
- Li NQ, Reddy PS, Thyagaraju K, Reddy AP, Hsu BL, Scholz RW, Tu CP, Reddy CC. Elevation of rat liver mRNA for selenium-dependentglutathione peroxidase by selenium deficiency. *J Biol Chem*. 1990; 265:108–13. [PubMed: 1688426]
- Lin CH, Tan EK, Chen ML, Tan LC, Lim HQ, Chen GS, Wu RM. Novel ATP13A2 variant associated with Parkinson disease in Taiwan and Singapore. *Neurology*. 2008; 71:1727–32. [PubMed: 19015489]
- Luk E, Yang M, Jensen LT, Bourbonnais Y, Culotta VC. Manganeseactivation of superoxide dismutase 2 in the mitochondria of *Saccharomyces cerevisiae*. *J Biol Chem*. 2005; 280:22715–20. [PubMed: 15851472]
- Miccadei S, Floridi A. Sites of inhibition of mitochondrial electron transportby cadmium. *Chem Biol Interact*. 1993; 89:159–67. [PubMed: 8269544]
- Moller AB, Asp T, Holm PB, Palmgren MG. Phylogenetic analysis of P5 P-type ATPases, a eukaryotic lineage of secretory pathway pumps. *Mol Phylogenet Evol*. 2008; 46:619–34. [PubMed: 18155930]

- Nisipeanu P, Kuritzky A, Korczyn AD. Familial levodopa-responsive parkinsonian-pyramidal syndrome. *Mov Disord.* 1994; 9:673–5. [PubMed: 7845409]
- Pearce DA, Sherman F. Toxicity of copper, cobalt, and nickel salts independent on histidine metabolism in the yeast *Saccharomyces cerevisiae*. *J Bacteriol.* 1999; 181:4774–9. [PubMed: 10438744]
- Perfus-Barbeoch L, Leonhardt N, Vavasseur A, Forestier C. Heavy metal toxicity: cadmium permeates through calcium channels and disturbs the plant water status. *Plant J.* 2002; 32:539–48. [PubMed: 12445125]
- Ramirez A, Heimbach A, Grundemann J, Stiller B, Hampshire D, Cid LP, Goebel I, Mubaidin AF, Wriekat AL, Roeper J, Al-Din A, Hillmer AM, Karsak M, Liss B, Woods CG, Behrens MI, Kubisch C. Hereditary parkinsonism with dementia is caused by mutations in *ATP13A2*, encoding a lysosomal type 5 P-type ATPase. *Nat Genet.* 2006; 38:1184–91. [PubMed: 16964263]
- Ravindranath SD, Fridovich I. Isolation and characterization of a manganese-containing superoxide dismutase from yeast. *J Biol Chem.* 1975; 250:6107–12. [PubMed: 238997]
- Rotruck JT, Pope AL, Ganther HE, Swanson AB, Hafeman DG, Hoekstra WG. Selenium: biochemical role as a component of glutathione peroxidase. *Science.* 1973; 179:588–90. [PubMed: 4686466]
- Schiestl RH, Gietz RD. High efficiency transformation of intact yeast cells using single stranded nucleic acids as a carrier. *Curr Genet.* 1989; 16:339–46. [PubMed: 2692852]
- Tandogan B, Ulusu NN. The inhibition kinetics of yeast glutathione reductase by some metal ions. *J Enzyme Inhib Med Chem.* 2007; 22:489–95. [PubMed: 17847717]
- Vida TA, Emr SD. A new vital stain for visualizing vacuolar membrane dynamics and endocytosis in yeast. *J Cell Biol.* 1995; 128:779–92. [PubMed: 7533169]
- Wang Y, Fang J, Leonard SS, Rao KM. Cadmium inhibits the electron transfer chain and induces reactive oxygen species. *Free Radic Biol Med.* 2004; 36:1434–43. [PubMed: 15135180]
- Weisiger RA, Fridovich I. Mitochondrial superoxide simutase. Site of synthesis and intramitochondrial localization. *J Biol Chem.* 1973; 248:4793–6. [PubMed: 4578091]
- Williams DR, Hadeed A, al-Din AS, Wriekat AL, Lees AJ. Kufor Rakeb disease: autosomal recessive, levodopa-responsive parkinsonism with pyramidal degeneration, supranuclear gaze palsy, and dementia. *Mov Disord.* 2005; 20:1264–71. [PubMed: 15986421]
- Zafar KS, Siddiqui A, Sayeed I, Ahmad M, Salim S, Islam F. Dose-dependent protective effect of selenium in rat model of Parkinson's disease: neurobehavioral and neurochemical evidences. *J Neurochem.* 2003; 84:438–46. [PubMed: 12558963]
- Zecca L, Youdim MB, Riederer P, Connor JR, Crichton RR. Iron, brain ageing and neurodegenerative disorders. *Nat Rev Neurosci.* 2004; 5:863–73. [PubMed: 15496864]

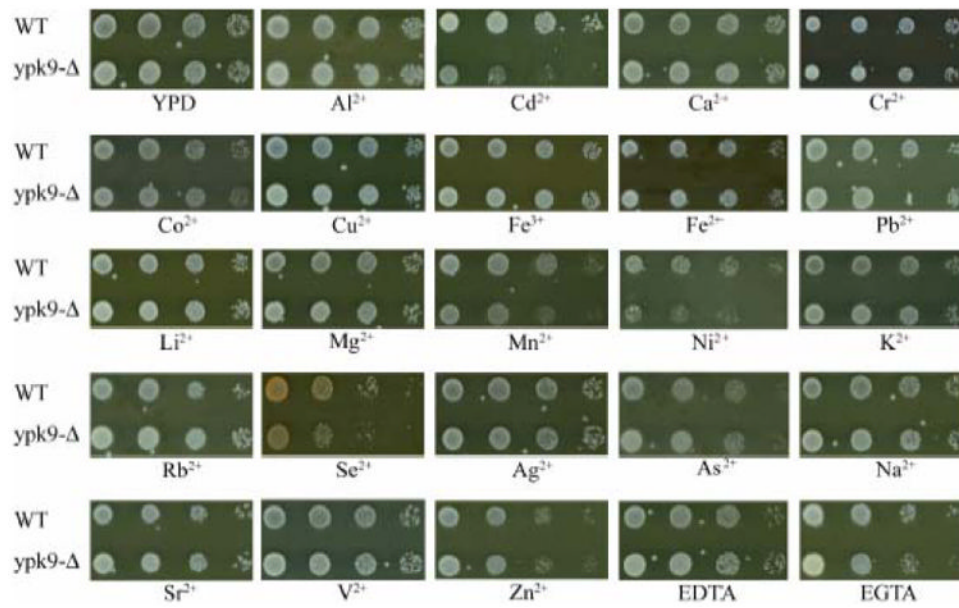


Figure 1. The deletion of *YPK9* confers sensitivity to cadmium, manganese, nickel and selenium
 Ten fold serial dilutions of wild-type and *ypk9-Δ* cells were plated on YPD media and media supplemented with metals at concentrations listed in Table I.

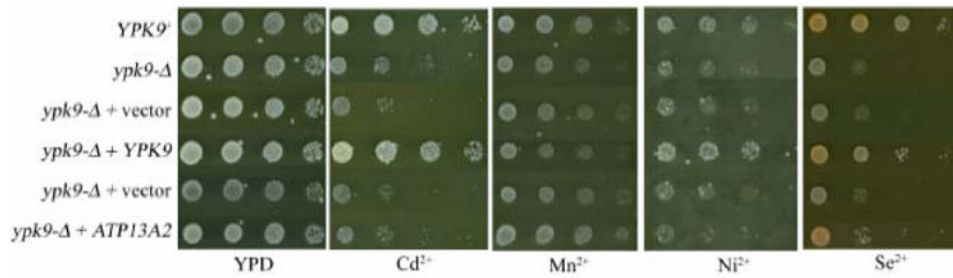


Figure 2. Expression of *YPK9* rescues cadmium, manganese, nickel and selenium sensitivity
Ten-fold serial dilutions of the listed strains were plated onto YPD media and media supplemented with cadmium, manganese, nickel and selenium at concentrations listed in Table I. *YPK9* expression, but not *ATP13A2* expression, restored growth in *ypk9-Δ* cells.

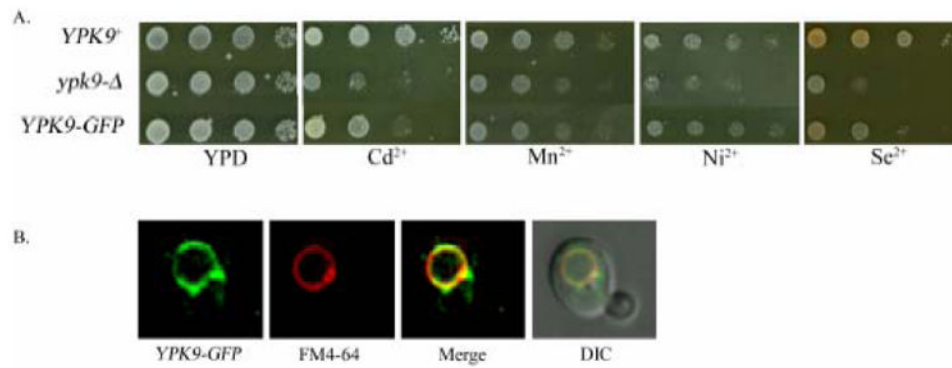


Figure 3. YPK9p localizes to the vacuole

The sterol dye FM4-64 was used to stain the vacuolar membrane. Colocalization of Ypk9-GFP with FM4-64 indicates vacuolar localization of Ypk9p. The GFP tagged protein maintains slight functionality in the cell, indicated by a resistance to cadmium, manganese, nickel and selenium compared to *ypk9-Δ*.

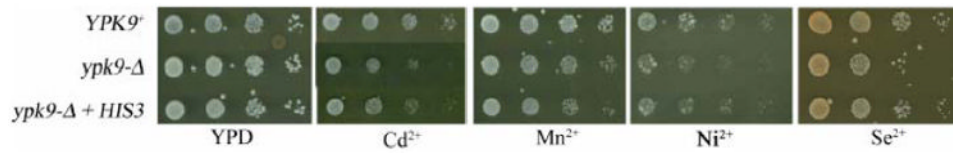


Figure 4. Histidine metabolism affects nickel and selenium toxicity in *ypk9-Δ*

The introduction of *HIS3* on a centromeric plasmid confers a complete histidine biosynthetic pathway in the strain used in this study and decreases the toxicity of nickel and selenium to *ypk9-Δ* cells.

Table I
Metal concentrations used for the screening of growth defects in *ypk9-Δ*

Metal salts were added to YPD and SC media at the corresponding sublethal level. All metal salt solutions were filter sterilized prior to use.

Metal	Final Concentration
Aluminum chloride	4.5 mM
Cadmium chloride	8 μ M
Calcium chloride	100 mM
Chromium chloride	8 mM
Cobalt chloride	1.2 mM
Copper sulfate	2.4 mM
Ferric chloride	5.5 mM
Ferrous chloride	7 mM
Lead chloride	2.5 mM
Lithium chloride	40 mM
Magnesium chloride	150 mM
Manganese chloride	3 mM
Nickel chloride	2.5 mM
Potassium chloride	540 mM
Rubidium chloride	5 mM
Selenium chloride	0.7 mM
Silver nitrate	0.35 mM
Sodium arsenic	2.5 mM
Sodium chloride	360 mM
Strontium chloride	2.25 mM
Vanadium oxide	13 mM
Zinc chloride	4.4 mM